Supporting Information

Experimental

Labeling of transferrin (Tf). A stock solution of Tf was prepared in PBS and purified using micro Bio-Spin chromatography columns (Bio-Rad, Hercules, USA). The molar concentration of Tf was measured spectrophotometrically using an extinction coefficient of 8.7×10^4 M^{-1} cm^{-1} at 280 nm. A stock solution of Atto647N-NHS-ester (ATTO-TEC, Siegen, Germany) was freshly prepared in anhydrous DMSO (dimethyl sulfoxide, Carl Roth, Karlsruhe, Germany) and stored at –18 ℃ in the dark before use. For dye conjugation, 250 μL of Tf solution (200 μM) was mixed with 174 μL PBS (Invitrogen, Carlsbad, CA), 26 μL Atto647N-NHS-ester (2.37 mM) and 50 μL $NaHCO_3$ solution (1 M), and incubated in the dark for 2 h at room temperature. Afterwards, unreacted dye and other small impurities were removed by a PD Miditrap G-25 column (GE Healthcare, Freiburg, Germany) using water as the eluent, and further concentrated with a Vivaspin 4 centrifugal concentrator (10 kDa, Sartorius, Göttingen, Germany) at 4 ℃. The degree of labeling (DOL, dye-to-protein ratio) was determined by absorption spectroscopy following the dye vendor's instructions. Under the current experimental conditions, the DOL was ca. 0.9. The purified Atto647N-Tf conjugate solution was stored in the dark at 4 ℃ before use.

Synthesis of Atto647N-Tf NPs. Tf NPs were synthesized by using a strategy modified from a previous report.[1] 1 mL unlabeled Tf solution (100 μM) in H_2O was mixed with 50 μL Atto647N-Tf (120 μM); thus, the ratio of dye to protein in the mixture solution was approximately 1:20. The pH of the solution was adjusted to 9.0 using 0.5 M NaOH solution. Under gentle stirring (500 rpm) at room temperature, acetone was added dropwise from a syringe until the solution became turbid. Subsequently, 50 μL of a 4% glutaraldehyde solution was added, and the solution was continuously stirred in the dark for 4 h. The as-obtained Tf NP solution was purified by removing acetone using a Vivaspin 15 Turbo centrifugal

concentrator (10 KDa, Sartorius). Then, the Tf NP-containing aqueous solution was passed through a PD 10 column (GE Healthcare) to remove free protein. Finally, the purified Atto647N-Tf NP solution was stored in the dark at 4 ℃ prior to use. Based on the hydrodynamic diameter of Tf NPs (44 ± 6 nm) and Tf (7 ± 1 nm) measured by DLS, the number of Tf per NP is estimated to be 248, assuming that all proteins are densely packed in the particles.

Characterization. Fluorescence emission spectra were taken on a Fluorolog-3 spectrofluorometer (HORIBA Jobin Yvon, Edison, NJ) with excitation at 470 nm. CD spectra were acquired on a J-815 CD spectrometer (JASCO Deutschland, Gross-Umstadt, Germany) with a 1 mm path length standard cell at 20 ℃ in the wavelength range 185 – 350 nm; each spectrum was an average of five scans. Fluorescence and CD spectra were corrected for buffer solution background. Dynamic light scattering (DLS) and laser Doppler anemometry (LDA) measurements were carried out on a Zetasizer Nano-ZS (Malvern Instruments, Malvern, UK) with a 633 nm He-Ne laser at 25 ℃. DLS data sets were taken at least in triplicate using a disposable UV microcuvette (Brand, Wertheim, Germany) and analyzed using number distributions; LDA measurements were carried out in a folded capillary ζ-potential cell (Malvern).

The morphology of NPs was investigated by high-angle annular dark-field scanning transmission electron microscopy (HAADF-STEM) performed on an FEI Osiris ChemiSTEM microscope (Eindhoven, The Netherlands) at 200 kV acceleration voltage. STEM samples were prepared by deposition of nanoparticles on a commercial holey amorphous carbon film, with a nominal thickness of 3 nm, at room temperature in air. The film is mounted on 400 μm mesh Cu grid. The composition and the distribution of different chemical elements within single nanoparticles was investigated by energy-dispersive X-ray spectroscopy (EDXS) elemental mapping performed on the FEI Osiris microscope at 200 kV by using a Bruker

Quantax system (XFlash detector). The EDXS maps were analyzed by using the ESPRIT software (version 1.9).

The concentration of Tf NPs was measured by dual-focus fluorescence correlation spectroscopy (Microtime 200, PicoQuant, Berlin, Germany) equipped with a water immersion objective (1.2 NA, 60×, Olympus, Hamburg, Germany).[2] The sample was excited by two orthogonally polarized pulsed 488 nm diode lasers (0.7 μW), and the fluorescence light, after passing through a band-pass filter (690/70 nm) and a pinhole (100 μm), was separated into two channels by a polarizing beam splitter and registered by avalanche photodiode detectors (SPCM-AQR-13, Perkin Elmer, Rodgau, Germany).

Cell culture and confocal imaging. HeLa cells were cultured in Dulbecco's modified Eagle's medium (DMEM, Invitrogen, Carlsbad, California), supplemented with 10% fetal bovine serum (FBS), 100 U of penicillin, and 100 μg/ml streptomycin in a humidified incubator at 37 °C and 5% CO_2. For fluorescence imaging to reveal the intracellular localization of Tf NPs, cells were seeded in eight-well LabTek™ chambers (Nunc, Langenselbold, Germany) and allowed to adhere overnight at 37 °C and 5% CO_2 before they were washed twice with PBS. Cells were incubated with 4 fM marker (CellLight Early Endosomes-GFP BacMam 2.0, Invitrogen) solution in culture medium for 16 h at 37 °C and 5% CO_2. After rinsing twice with PBS, cells were exposed to 1 nM Tf NPs in serum-free DMEM for 2 h and washed twice with PBS to remove free NPs. Afterwards, cells were cultured and imaged in DMEM with 10% FBS. Images were acquired by using an Andor Revolution® XD spinning disk confocal laser scanning microscopy system (BFi OPTiLAS, München, Germany).[3] Tf NPs were excited at 640 nm; their emission was collected through a bandpass filter (685/40 nm, AHF, Tübingen, Germany). The endosome marker was excited at 488 nm, and the emission was collected through a bandpass filter (565/54 nm, center wavelength/width, AHF).

For mechanistic uptake studies, cells were pretreated for 30 min with 10 μM chlorpromazine hydrochloride or 20 μM Tf in serum free DMEM. Subsequently, Atto647N

Tf NPs at a final concentration of 1 nM was added to the serum free DMEM containing chlorpromazine (10 μM) or Tf (20 μM) and incubated with cells for 2 h. Afterwards, cell membranes were stained with CellMask™ green (Invitrogen) in DMEM for 5 min. The cells were thoroughly washed twice with PBS before imaging. For quantitative analysis, the fluorescence images were analyzed using Image J. The fluorescence intensity of NPs of each cell was obtained by dividing the integrated intensity by the cell area. To assess NP colocalization with cell organelle markers, Manders's overlap coefficient was calculated. Specifically, only NPs with Manders's coefficient not less than 0.5 were considered to overlap well with the relevant organelle structures.[4] When calculating the fraction of colocalized Tf NPs, the fluorescence emission intensity was taken to reflect the amount of NPs.

Viability and proliferation of HeLa cells upon treatment with Tf NPs was evaluated by measuring the metabolic activity of cells using an MTT assay as previously described.[5] Particularly, HeLa cells were incubated in 1 nM Atto647N-Tf NPs in DMEM medium for 2 h for measuring proliferation. After washing with PBS twice, the cells were further incubated in DMEM with 10% FBS at 37 ℃ and 5% CO_2. Afterwards, MTT assays were carried out every 24 h to monitor cell proliferation. For comparison, control experiments were performed by using non-treated cells.

STED imaging. STED experiments were performed on a custom-built STED microscope, which was modified from a recently published design (Scheme S1).[6] Excitation light was generated by a 640-nm pulsed diode laser (LDH-PC-640B, PicoQuant), emitting 100-ps pulses at 80 MHz. The excitation light was spectrally filtered by a 640/14 nm bandpass and spatially cleaned by 2 m of single-mode polarization-maintaining fiber (PMJ-A3HPC, OZ Optics, Ottawa, Canada). The depletion light was delivered by an 80-MHz mode-locked Ti:Sa laser (Mai Tai HP; Newport Spectra-Physics, Darmstadt, Germany) tuned to 780 nm. The 100-fs pulses of the Ti:Sa laser were stretched to 300 ps by a 60-cm long SF6 glass rod and 100 m of polarization maintaining single mode fiber (PMJ-A3HPC, OZ Optics, Ottawa,

Canada). Stretching ensures complete temporal coverage of the excitation pulse by the STED pulse to efficiently suppress spontaneous emission of the fluorophores. In addition, the lower photon density of the STED pulse reduces re-excitation and photodamage via multi-photon processes.

To create a doughnut-shaped focus to sharpen the region from which fluorescence emanates, a vortex phase mask was loaded onto a spatial light modulator SLM (LETO, HOLOEYE Photonics AG, Berlin, Germany). The phase mask was superimposed with a blazed grating to exclude non-modulated components of the reflected beam. Excitation and depletion beams were passed through a beam scanner (Yanus IV, Till Photonics, Germany) and a quarter-wave plate, and focused by a microscopic objective (HCX PL APOCS X100/1.46; Leica, Wetzlar, Germany) onto the sample. Fluorescence light was collected by the same objective, separated by a quad-band dichroic mirror (zt405/488/561/640rpc; Chroma Technology Corp, Bellows Falls) and focused into a multimode fiber in lieu of a confocal pinhole, with a core diameter corresponding to one Airy unit. Subsequently, the fluorescence was filtered by a 676/37 nm bandpass filter (HC 676/37, Semrock, Rochester, NY) to block scattered excitation and STED photons. Photons were detected by an avalanche photodiode (τ-SPAD-50; PicoQuant) and registered by a data acquisition card (PCI-6259; National Instruments, Munich, Germany). The excitation power was 4.4 μW at the sample, and the power of the depletion beam at the sample was 28 mW. STED Images were taken by raster scanning the sample with a pixel size of 20 nm and pixel dwell time of 40 μs. Confocal images were taken with identical settings right after the STED images.

Calculation of the resolution of microscopy. The resolution of both STED and confocal microscopy by using our sriNPs was calculated via the equation

$$r = (D_m^2 - D_a^2)^{1/2}, \quad (1)$$

where r is the optical resolution of the microscope, D_m is the object diameter measured in the image, and D_a is the real object diameter. The size of punctate structures (endosomes) inside

the cells upon NP internalization, 164 nm, was also calculated with this equation, using values 64 nm and 176 nm for r and D_m, respectively. Thus, the number of sriNPs (diameter: 44 nm) within each vesicle (diameter: 164 nm) was estimated as 52, assuming dense NP packing within the vesicles.

Brightness comparision of sriNPs and free Atto647N. Single Atto647N dye molecules and sriNPs were immobilized on glass surfaces and imaged by our home-made STED microscope (with STED power set to 0) described in Figure S1. The power and pixel dwell time of the 640-nm excitation laser were set to 7.5 μW and 40 μs, respectively. A rectangular area (20 × 20 μm^2) was scanned repeatedly to collect 1000 image frames of 200 × 200 pixels from each sample, after which all fluorophores were bleached. The two image sets were integrated to yield a single 2D image for each sample. Fluorophores and NPs were identified by segmentation, and the intensities within areas containing a single fluorescent dye or NP were integrated. From these data, histograms were compiled of the number of dyes and NPs, for which a specific number of photons was registered (Figure S9). The averages over these distributions, 132,000 (sriNPs) and 30,000 (dyes) photons, reveal that each sriNP contains multiple dye molecules and emits more than four times the number of photons per unit time in comparison to the bare dye, so that faster image sequences (shorter pixel dwell times) are possible without sacrificing image quality.

Scheme and figures

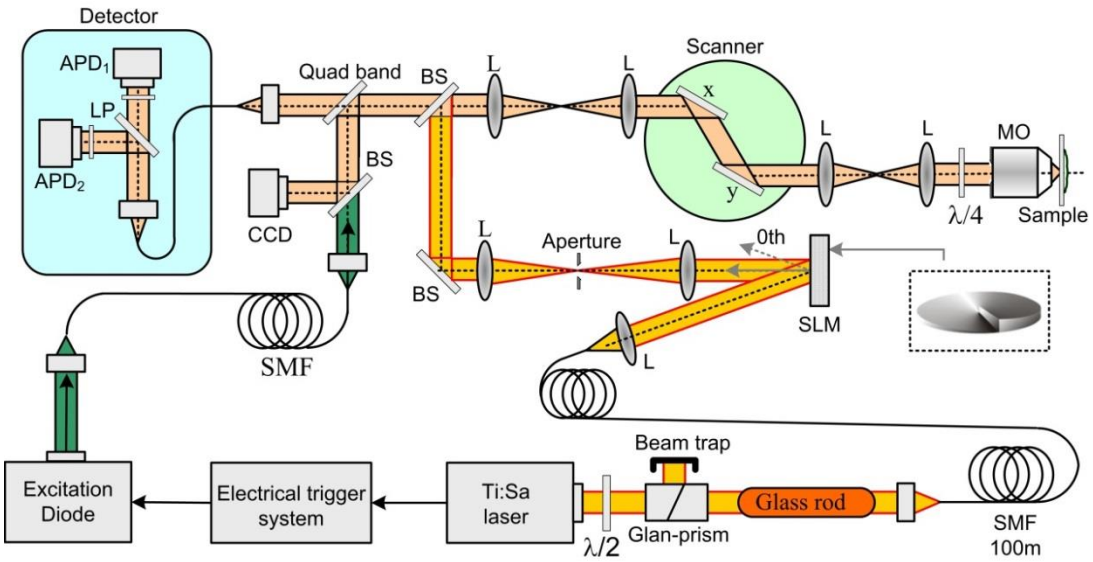

Scheme S1 Schematic illustration of our STED microscope used in this study.

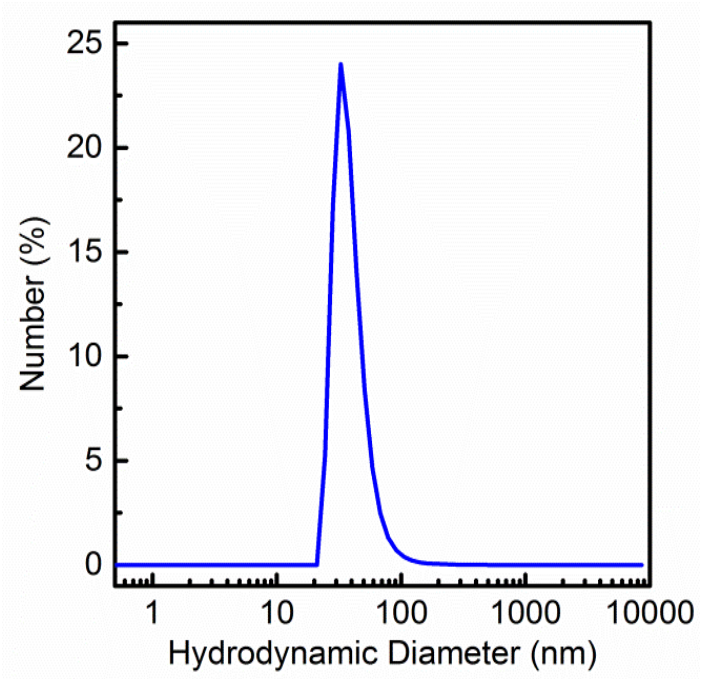

Figure S1 Size distribution of Atto647N-Tf NPs in PBS as determined by DLS.

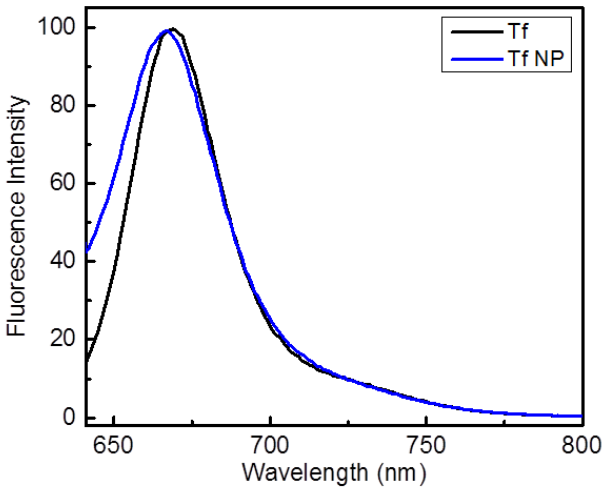

Figure S2 Fluorescence emission spectra of Atto647N-Tf (black) and Atto647N-Tf NPs (blue) in PBS, taken with excitation at 640 nm.

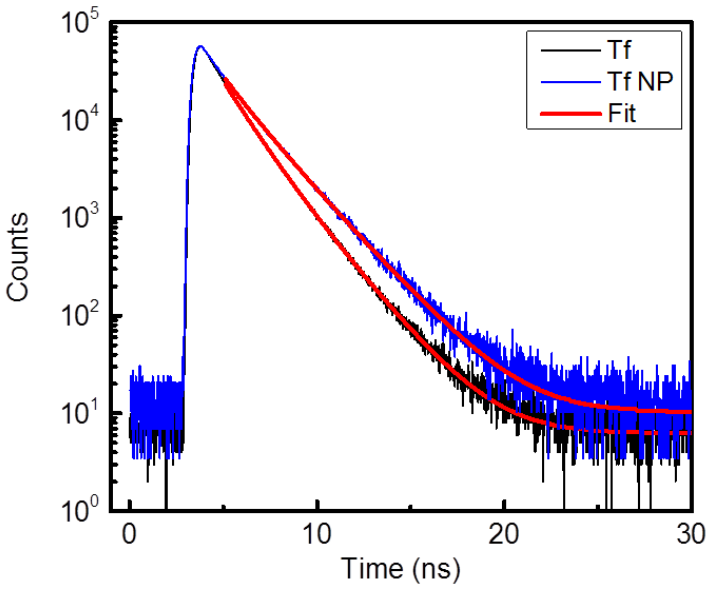

Figure S3 Fluorescence decay of Atto647N-Tf (black) and Atto647N-Tf NPs (blue) in PBS upon excitation at 640 nm. The red curves represent single exponential fits of the data.

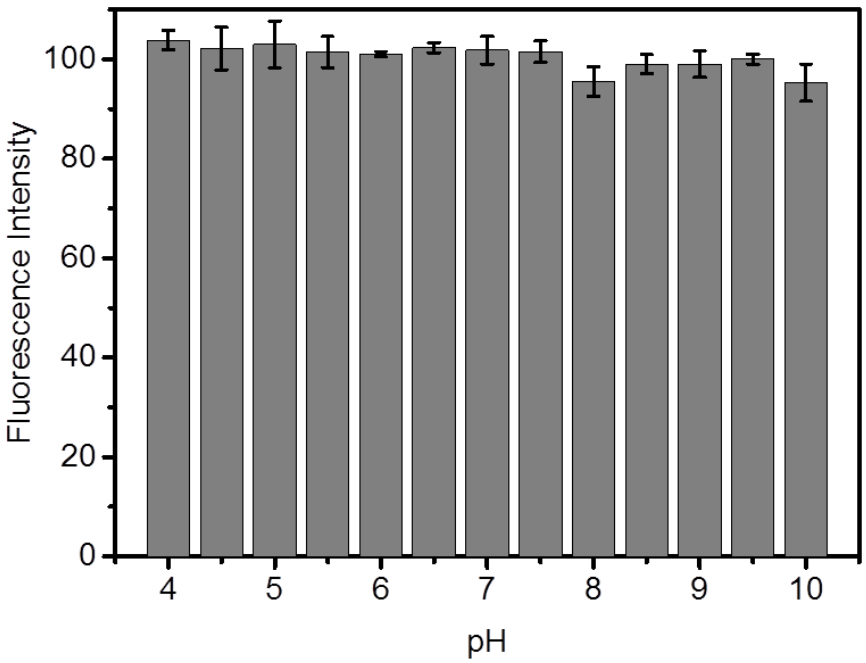

Figure S4 Dependence of the fluorescence intensity of Atto647N-Tf NPs in PBS solution on pH.

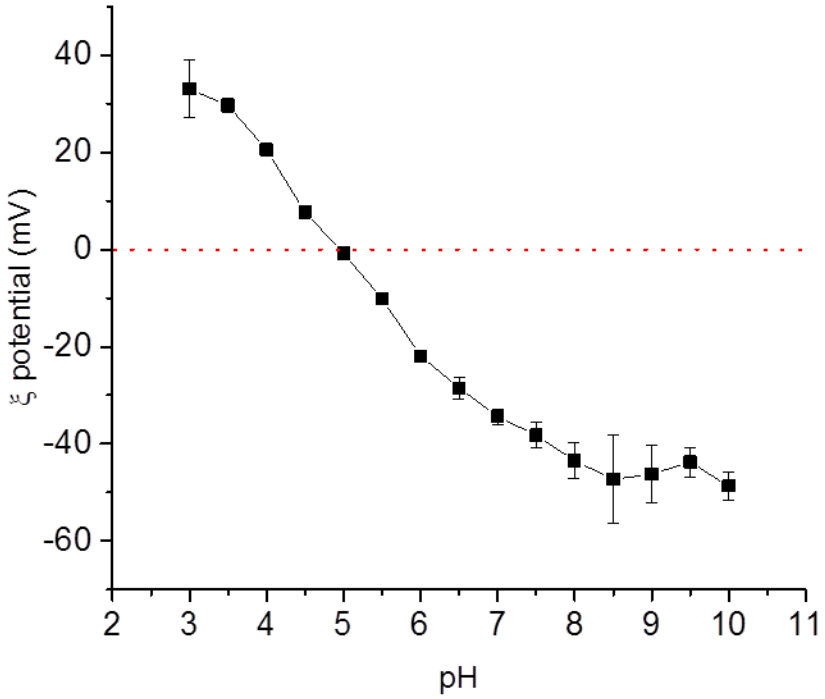

Figure S5 ζ-potential of Atto647N-Tf NPs in PBS, plotted as a function of pH. The error bars denote the standard deviation from at least six independent measurements.

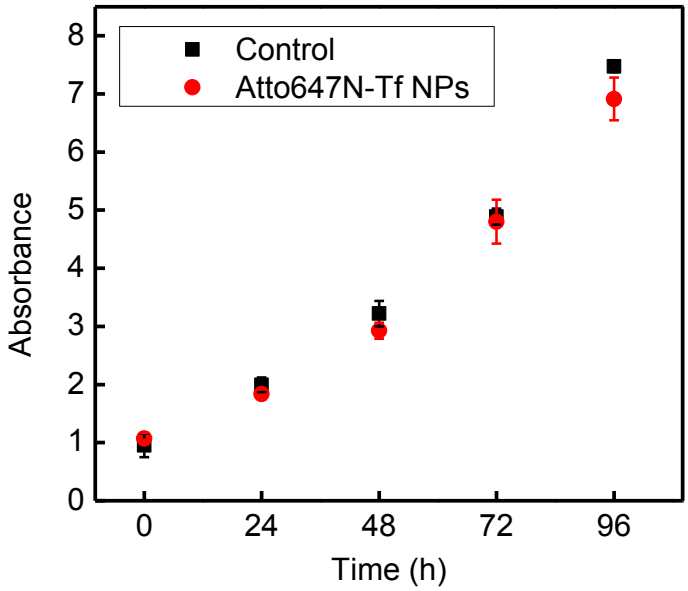

Figure S6 Proliferation assay of HeLa cells incubated with Atto647N-Tf NPs (1 nM, red) and control measurement (black) for comparison. The error bars denote the standard deviation from four independent measurements.

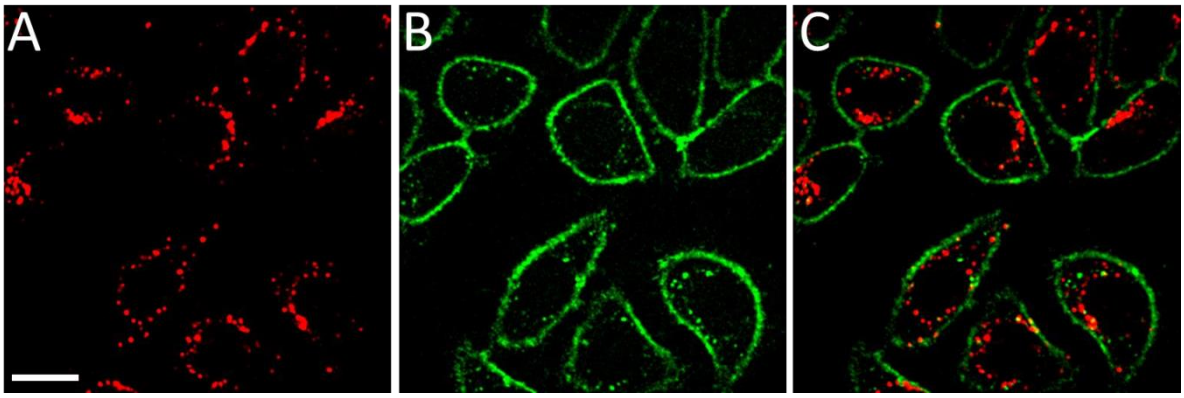

Figure S7 Typical confocal images of HeLa cells after incubation with 1 nM Atto647N-Tf NPs for 2h in DMEM: (A) NPs, in red; (B) plasma membrane stained by CellMask Green, in green; (C) overlay of the red and green channels. Scale bar, 20 μm.

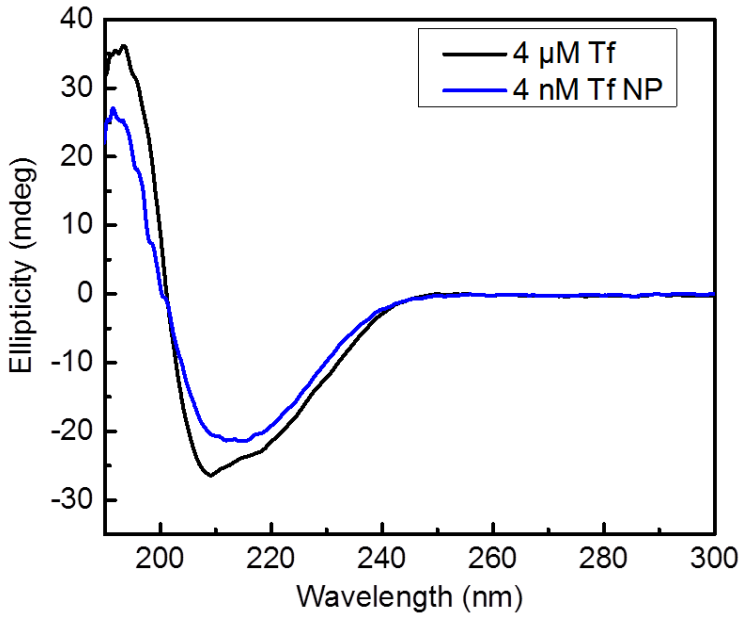

Figure S8 CD spectra of Tf (black) and Atto647N-Tf NPs (blue) in PBS. The different far-UV CD spectra indicate that the secondary structure of Tf is modified to a certain extent if the protein is part of the NP assembly.

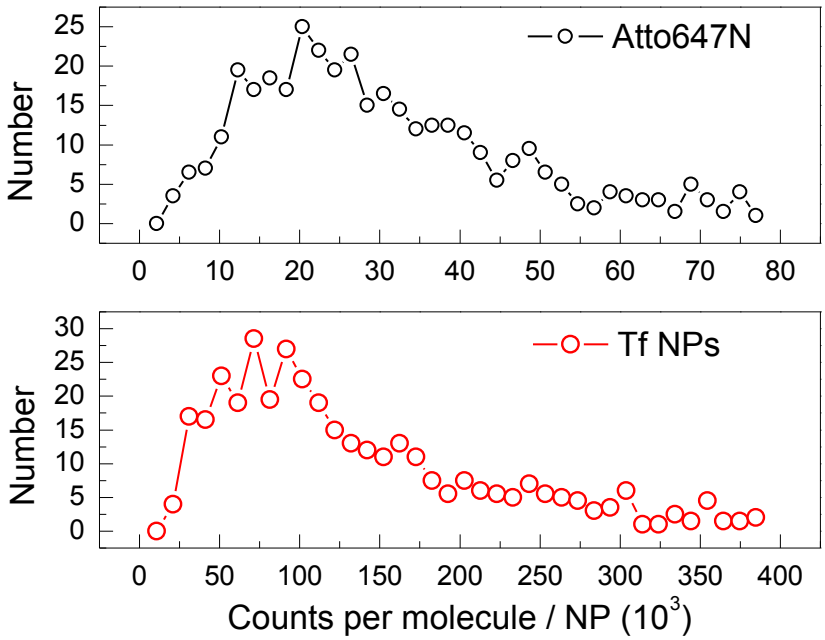

Figure S9 Histograms of the numbers of single Atto647N molecules (black) and Atto647N-Tf NPs (red), binned according to the number of photons registered for each, using identical imaging conditions.

References

1. W. Lin, A. Coombes, M. Davies, S. Davis and L. Illum, *J. Drug Target.*, 1993, **1**, 237-243.
2. P. Maffre, K. Nienhaus, F. Amin, W. J. Parak and G. U. Nienhaus, *Beilstein J. Nanotechnol.*, 2011, **2**, 374-383.
3. L. Shang, L. Yang, F. Stockmar, R. Popescu, V. Trouillet, M. Bruns, D. Gerthsen and G. U. Nienhaus, *Nanoscale*, 2012, **4**, 4155-4160.
4. L. Yang, L. Shang and G. U. Nienhaus, *Nanoscale*, 2013, **5**, 1537-1543.
5. L. Shang, L. Yang, J. Seiter, M. Heinle, G. Brenner-Weiss, D. Gerthsen and G. U. Nienhaus, *Adv. Mater. Interfaces*, 2014, **1**, 1300079.
6. P. N. Hedde, R. M. Dörlich, R. Blomley, D. Gradl, E. Oppong, A. C. B. Cato and G. U. Nienhaus, *Nat. Commun.*, 2013, **4**, 2093.